

Femtosecond dynamics of relaxation of photoexcited *meso*-tetraferrocenylporphyrin in the nonprotonated and diprotonated forms (Fc_4PH_2 and $\text{Fc}_4\text{PH}_4^{2+}$)

V. A. Nadtochenko,^{a*} D. V. Khudyakov,^a N. V. Abramova,^b E. V. Vorontsov,^b N. M. Loim,^b
F. E. Gostev,^c D. G. Tovbin,^c A. A. Titov,^c and O. M. Sarkisov^c

^aInstitute of Problems of Chemical Physics, Russian Academy of Sciences,
14 Institutskii prosp., 142432 Cherogolovka, Moscow Region, Russian Federation.

Fax: +7 (096) 515 3588. E-mail: nadto@icp.ac.ru

^bA. N. Nesmeyanov Institute of Organoelement Compounds, Russian Academy of Sciences,
28 ul. Vavilova, 119991 Moscow, Russian Federation.

Fax: +7 (095) 135 5085. E-mail: stemos@inios.ac.ru

^cN. N. Semenov Institute of Chemical Physics, Russian Academy of Sciences,
4 ul. Kosygina, 119991 Moscow, Russian Federation.

Fax: +7 (095) 137 8284

The relaxation of the $Q^1(\pi-\pi^*)$ excited state of the nonprotonated Fc_4PH_2 and diprotonated $\text{Fc}_4\text{PH}_4^{2+}$ forms of *meso*-tetraferrocenylporphyrin was studied by femtosecond laser absorption spectroscopy. Transition from the $Q^1(\pi-\pi^*)$ state to the charge-transfer state was shown to occur within 208 ± 10 fs for Fc_4PH_2 and 9 ± 3 ps for $\text{Fc}_4\text{PH}_4^{2+}$. A fast vibrational relaxation with a characteristic time of 120–140 fs was found for both forms. The relaxation time of $\text{Fc}^{\delta+}-\text{P}^{\delta-}$ charge-transfer state for Fc_4PH_2 was 17 ± 4 ps.

Key words: femtosecond dynamics, porphyrins, *meso*-metalloenylporphyrins, charge-transfer state.

Molecular systems based on electron-donor or electron-acceptor molecules covalently linked to the porphyrin ring are convenient models for studying the directed electron transfer in biological electron-transport chains.^{1–3} These systems are of interest for optoelectronics^{4,5} and biomedicine,⁶ for the development of photocatalytic^{1–3} and photogalvanic⁷ light energy converters.

A new class of porphyrins, *viz.*, *meso*-metalloenylporphyrins, was recently synthesized.^{8,9} Based on the data obtained by steady-state and nanosecond laser photolyses on the photochemical properties of *meso*-tetraferrocenylporphyrin (Fc_4PH_2), we assumed that a charge-transfer state, whose energy is lower than that of the $^1(\pi-\pi^*)$ state, plays the determining role in the relaxation of the excited state of Fc_4PH_2 .¹⁰

The purpose of this work is to study the dynamics of relaxation of Fc_4PH_2 and its diprotonated form ($\text{Fc}_4\text{PH}_4^{2+}$) by femtosecond absorption laser kinetic spectroscopy. Since the differential absorption spectra of the $^1(\pi-\pi^*)$ and $^3(\pi-\pi^*)$ excited states and radical π -anions and π -cations are similar in a wide spectral range for the most part of porphyrins,¹¹ comparative analysis of the dynamics of relaxation of the nonprotonated and diprotonated forms of Fc_4PH_2 makes it possible to reveal the sequence of relaxation transitions in more detail.

Experimental

The experimental setup for studying the femtosecond dynamics of excited states has previously been described.¹² In this work, excitation was performed by the main harmonic of a dye laser ($\lambda = 610$ nm) with a pulse duration at the half-width of 50 fs. The experiment was conducted in the excitation–probing scheme. The polarization of the excitation and probing light was oriented at the magic angle. For probing the light from the femtosecond continuum was used, which was excited in an $\text{H}_2\text{O}-\text{D}_2\text{O}$ (50 : 50) mixture by the main harmonic pulse. The differential absorption spectra were recorded in the spectral window $\lambda = 380-590$ nm by a couple of diode arrays. The upper time limit was 20 ps.

Absorption spectra were measured on Hewlett–Packard 8452 diode-array and Specord M-40 spectrophotometers with digital data recording. Fluorescence spectra were measured on an Elyumin fluorimeter at 296 K. ^1H NMR spectra were recorded on a Bruker 400 HX spectrometer in CDCl_3 .

Syntheses and purification of Fc_4PH_2 , *meso*-tetra $rutheno$ -enyl- (Rc_4PH_2) and *meso*-tetracy $mantrenyl$ porphyrins (Cym_4Ph_2) have previously been described.^{8,9} Perchloric acid (Fluka), MeCN for chromatographic analysis (Fluka) purified by a standard procedure, and CHCl_3 (specially pure grade) were used. Solutions of porphyrins with a concentration of $(2-3) \cdot 10^{-5}$ mol L^{-1} were prepared in a CHCl_3 –MeCN (50 : 50 (vol.%)) mixture. No effect of the air oxygen on the

spectra of solutions was observed when the contact time with air did not exceed 5–8 h. Uncontrolled spectral changes occurred upon a longer contact.

Results and Discussion

The quantum yield of fluorescence of Fc_4PH_2 ($\phi_{\text{Fc}_4\text{PH}_2}$) was measured relatively to the fluorescence of tetraphenylporphyrin (H_2TPP). It was found that at 296 K $\phi_{\text{Fc}_4\text{PH}_2} \leq 10^{-5} \phi_{\text{H}_2\text{TPP}}$. The lifetime of the $\text{Q}^1(\pi-\pi^*)$ state of the H_2TPP molecule is 10 ns.¹³ Taking equal the rate constants of the radiative transitions of the $^1(\pi-\pi^*)$ state for Fc_4PH_2 and H_2TPP , the time of nonradiative relaxation of Fc_4PH_2 should be about 0.1 ps. The low quantum yield of Fc_4PH_2 fluorescence indicates relaxation processes in the femtosecond time interval.

The addition of protic acids (CCl_3COOH , CF_3COOH , and HClO_4) to a solution of Fc_4PH_2 results in the formation of the diprotonated porphyrin $\text{Fc}_4\text{PH}_4^{2+}$, which is indicated by changes in the absorption and ^1H NMR spectra (Figs. 1 and 2). In the case of CCl_3COOH , at the ratio porphyrin : acid $< 1 : 2.4$ the ^1H NMR spectrum simultaneously exhibits signals from both the nonprotonated and diprotonated forms, whereas

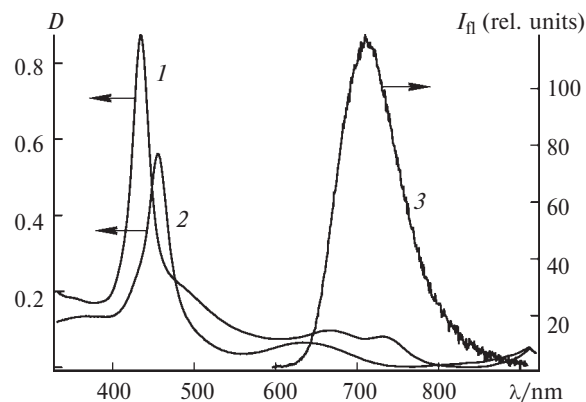


Fig. 1. Absorption spectra for Fc_4PH_2 (1) and $\text{Fc}_4\text{PH}_4^{2+}$ (2) and fluorescence spectrum for $\text{Fc}_4\text{PH}_4^{2+}$ (3) in MeCN at 296 K.

only the spectrum of $\text{Fc}_4\text{PH}_4^{2+}$ is observed when the ratio is increased to 1 : 7. When a concentration is HClO_4 of $1 \cdot 10^{-3} \text{ mol L}^{-1}$, *meso*-tetraferrocenylporphyrin exists almost completely in the $\text{Fc}_4\text{PH}_4^{2+}$ form. The $\text{Fc}_4\text{PH}_4^{2+}$ compound (see Fig. 1) manifests a more intense fluorescence than the nonprotonated form, and the quantum yield is $\phi_{\text{Fc}_4\text{PH}_4^{2+}} = 9 \cdot 10^{-4} \phi_{\text{H}_2\text{TPP}}$. This fact indicates at

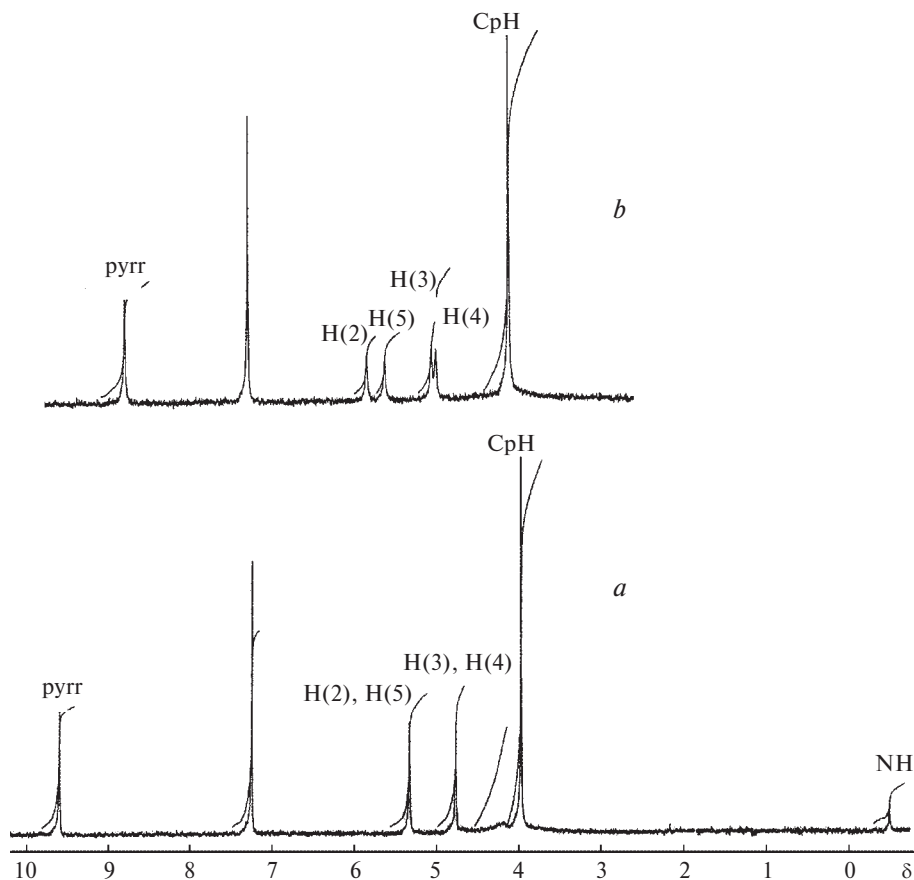


Fig. 2. ^1H NMR spectra of a solution of Fc_4PH_2 in CDCl_3 in the absence (a) and presence of CCl_3COOH (3 mol. eq.) (b).

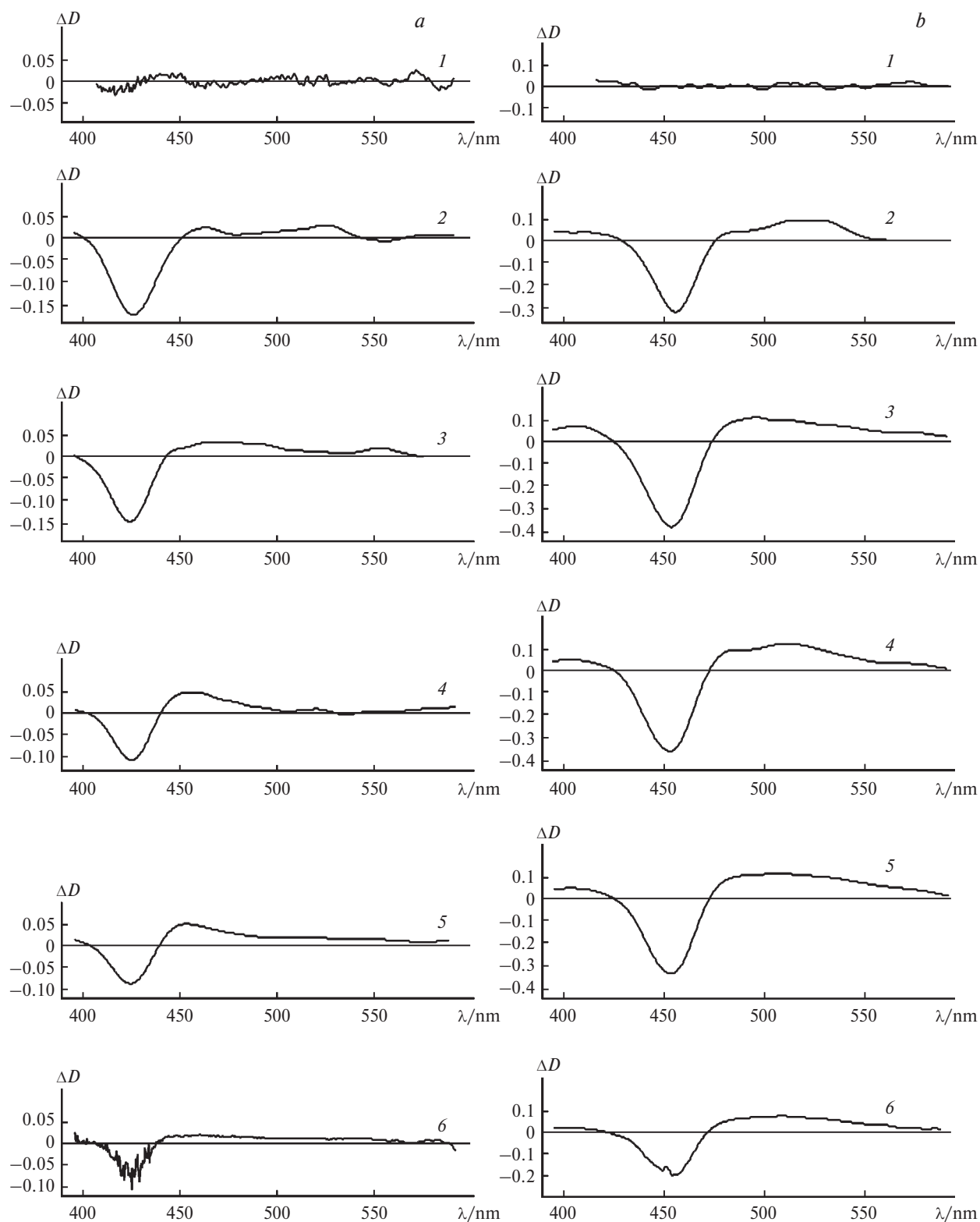


Fig. 3. Differential spectra for the excitation of Fc_4PH_2 ($2 \cdot 10^{-5} \text{ mol L}^{-1}$) (a) and $\text{Fc}_4\text{PH}_4^{2+}$ ($3 \cdot 10^{-5} \text{ mol L}^{-1}$) (b) with the light pulse with $\lambda = 610 \text{ nm}$ in a $\text{CHCl}_3\text{--MeCN}$ (50 : 50, vol.%) solution at 296 K and response times of -200 (1), 0 (2), 150 (3), 600 fs (4), 1.8 (5), and 20 ps (6).

least a 100-fold decrease in the rate of nonradiative relaxation of the $\pi-\pi^*$ system in the diprotonated form of ferrocenylporphyrin compared to that of the nonprotonated form if we accept that the rate constants of the radiative $^1(\pi-\pi^*)$ transition for Fc_4PH_2 and $\text{Fc}_4\text{PH}_4^{2+}$ are approximately the same.

The wavelength of the femtosecond pulse (610 nm) is in the region of Q absorption bands of the porphyrin ring for both diprotonated and nonprotonated forms. Therefore, $Q^1(\pi-\pi^*)$ is their initial excited state. The experimental data reflecting the relaxation processes from the $Q^1(\pi-\pi^*)$ state are presented in Figs. 3–7.

The differential spectra of both porphyrin forms Fc_4PH_2 and $\text{Fc}_4\text{PH}_4^{2+}$ (see Fig. 3) contain intense decay bands, which virtually coincide in position with the corresponding B absorption bands of the ground state of Fc_4PH_2 or $\text{Fc}_4\text{PH}_4^{2+}$. The decay signal is due to the fact that the molar absorptivity of the B band of the ground state is usually much greater than that for the excited $\pi\pi^*$ state or the π -radical ions of substituted porphyrins.¹¹ Similar decay is also observed for the nonsubstituted porphyrin when the Q band is excited, which agrees qualitatively with the assumption about the initial $Q^1(\pi-\pi^*)$ state for Fc_4PH_2 or $\text{Fc}_4\text{PH}_4^{2+}$. In addition, broad absorption bands at 440–570 and 470–590 nm were detected in the spectra of Fc_4PH_2 and $\text{Fc}_4\text{PH}_4^{2+}$, respectively. In the case of Fc_4PH_2 , a noticeable spectral narrowing of the absorption band at $\lambda = 440\text{--}570$ nm is observed with time ($t < 600$ fs) to $\lambda = 440\text{--}500$ nm (see Fig. 3, a). This fact can be an indication of the intramolecular charge transfer from Fc to the porphyrin ring because the absorption band of the porphyrin π -radical anions in this spectral region is narrower than the band of the $^1(\pi-\pi^*)$ state and has a maximum at ~ 450 nm.¹¹

The following transition processes can be distinguished in the differential absorption curves for Fc_4PH_2 and $\text{Fc}_4\text{PH}_4^{2+}$ (see Figs. 4–7).

1. The front edge of the decay curves, namely, 425 nm for Fc_4PH_2 (see Fig. 4) and 440 nm for $\text{Fc}_4\text{PH}_4^{2+}$ (see Fig. 5), and the corresponding absorption curves (450 nm (see Fig. 4) and 485 nm (see Fig. 5)) exhibit the growth of the signal amplitude approximated by the function $A[1 - \exp(-t/\tau)]$ with the characteristic time $\tau = 125 \pm 30$ fs. For comparison, the front edges of the curves for 435 and 465 nm are shown in Figs. 4 and 5, which reflects the time resolution of experiment (the fronts are approximated by the function $A[1 - \exp(-t/\tau)]$ with $\tau = 50$ fs). These facts indicate the existence of a relaxation process with 125 ± 30 fs.

2. At longer times, the nonprotonated Fc_4PH_2 form exhibits the decay of the amplitude of the signal with the time approximated by the function $[A\exp(-t/\tau) + B]$ (see Fig. 4, a, b) with $\tau = 208 \pm 10$ fs. It is important that a similar fast relaxation component (with a time of ~ 200 fs) is not observed for the diprotonated $\text{Fc}_4\text{PH}_4^{2+}$ porphyrin.

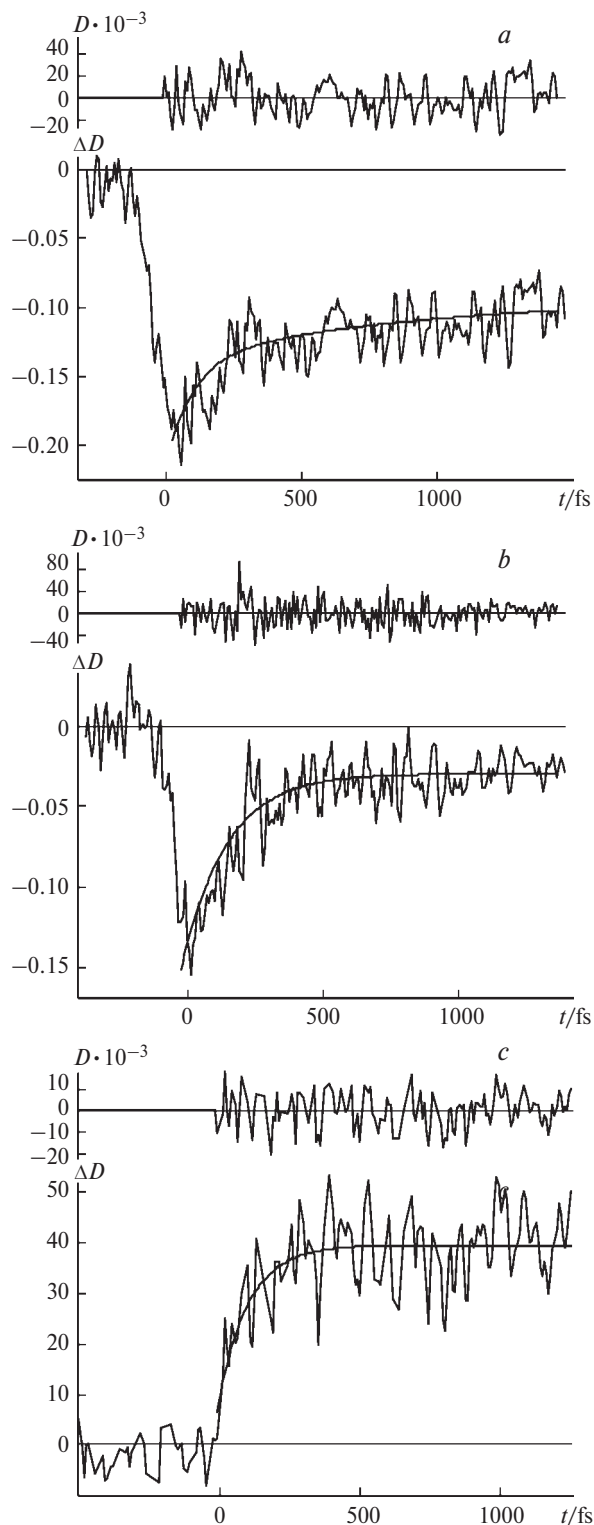


Fig. 4. Relaxation absorption curves in the femtosecond time scale upon the excitation of Fc_4PH_2 ($2 \cdot 10^{-5}$ mol L^{-1}) in a $\text{CHCl}_3\text{--MeCN}$ (50 : 50, vol.%) solution at 296 K: $\lambda = 425$ (a), 435 (b), and 450 nm (c). The results of approximation of the curves with the corresponding exponential functions are presented.

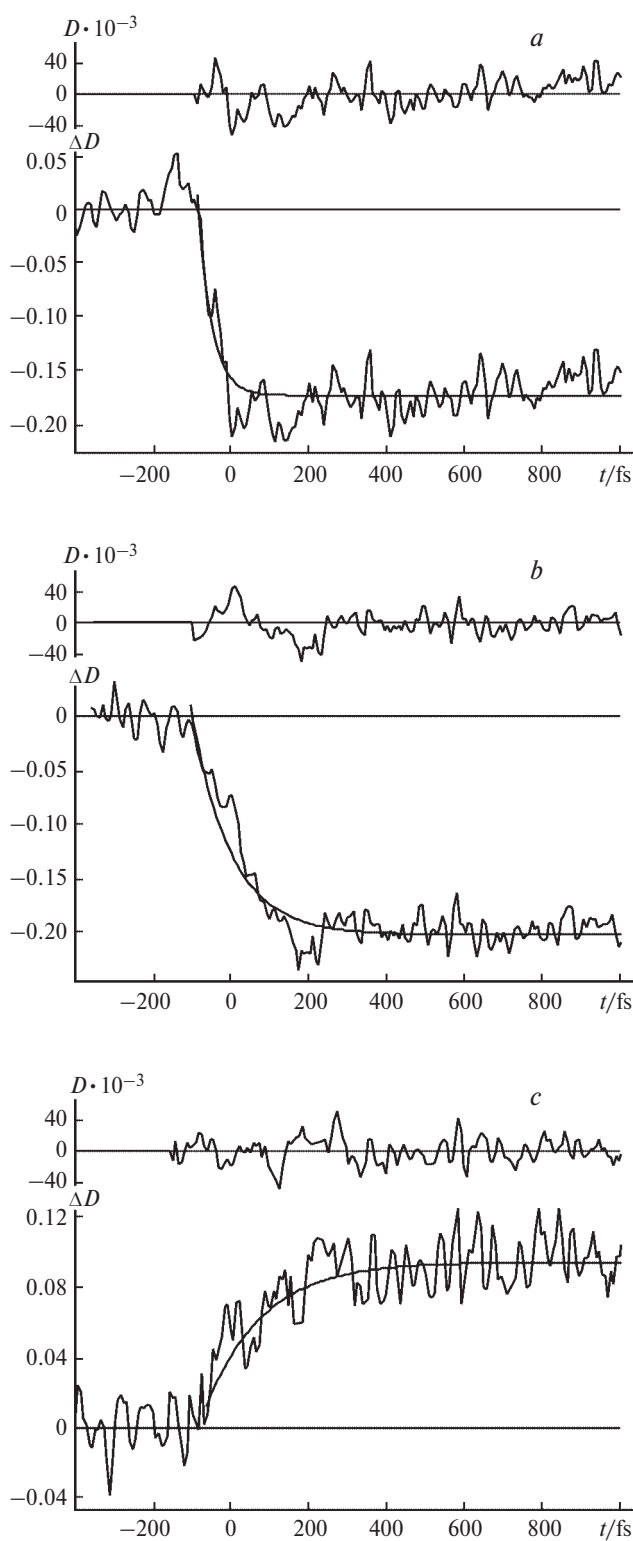


Fig. 5. Relaxation absorption curves in the femtosecond time scale upon the excitation of $\text{Fc}_4\text{PH}_4^{2+}$ ($3 \cdot 10^{-5} \text{ mol L}^{-1}$) in a CHCl_3 – MeCN (50 : 50, vol.%) solution at 296 K: $\lambda = 465$ (a), 440 (b), and 480 nm (c). The concentration of HClO_4 is $1 \cdot 10^{-3} \text{ mol L}^{-1}$. The results of approximation of the curves with the corresponding exponential functions are presented.

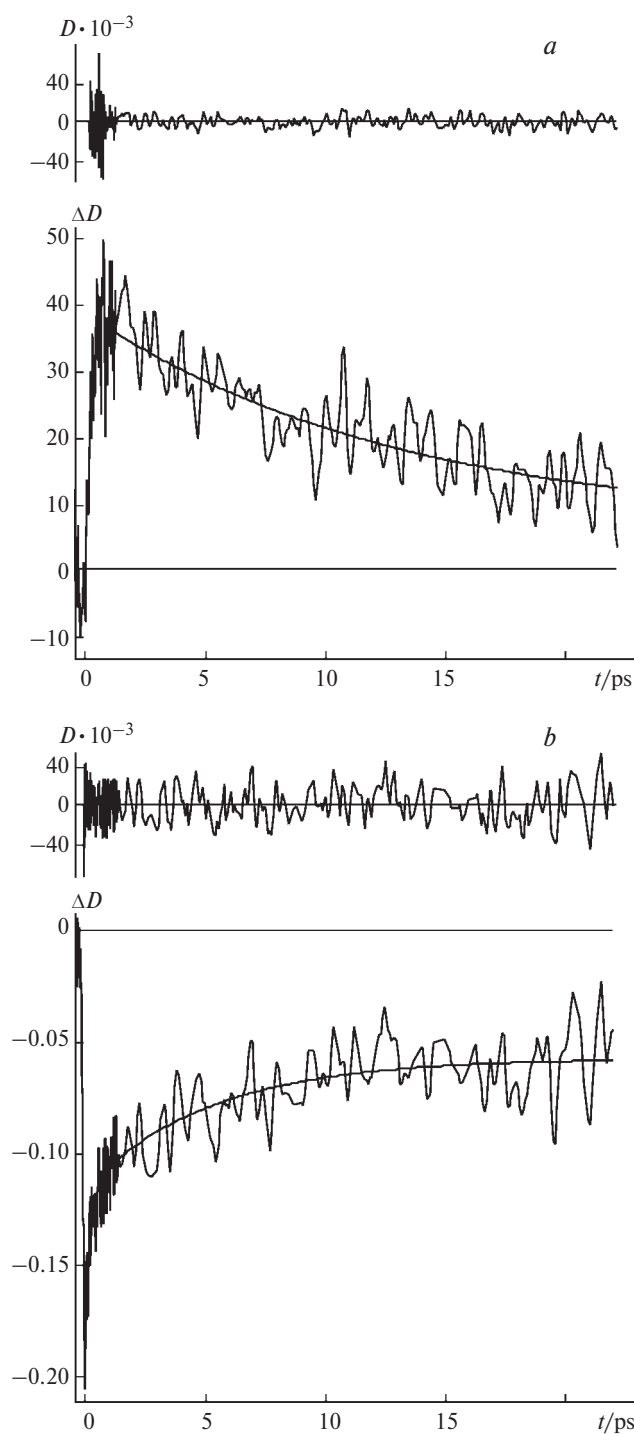


Fig. 6. Relaxation absorption curves in the picosecond time scale upon the excitation of Fc_4PH_2 ($2 \cdot 10^{-5} \text{ mol L}^{-1}$) in a CHCl_3 – MeCN (50 : 50, vol.%) solution at 296 K: $\lambda = 445$ (a) and 425 nm (b). The results of approximation of the curves with the corresponding exponential functions are presented.

3. In the picosecond time scale in the time interval ≤ 20 ps, the relaxation of the nonprotonated Fc_4PH_2 and diprotonated $\text{Fc}_4\text{PH}_4^{2+}$ forms is described by differ-

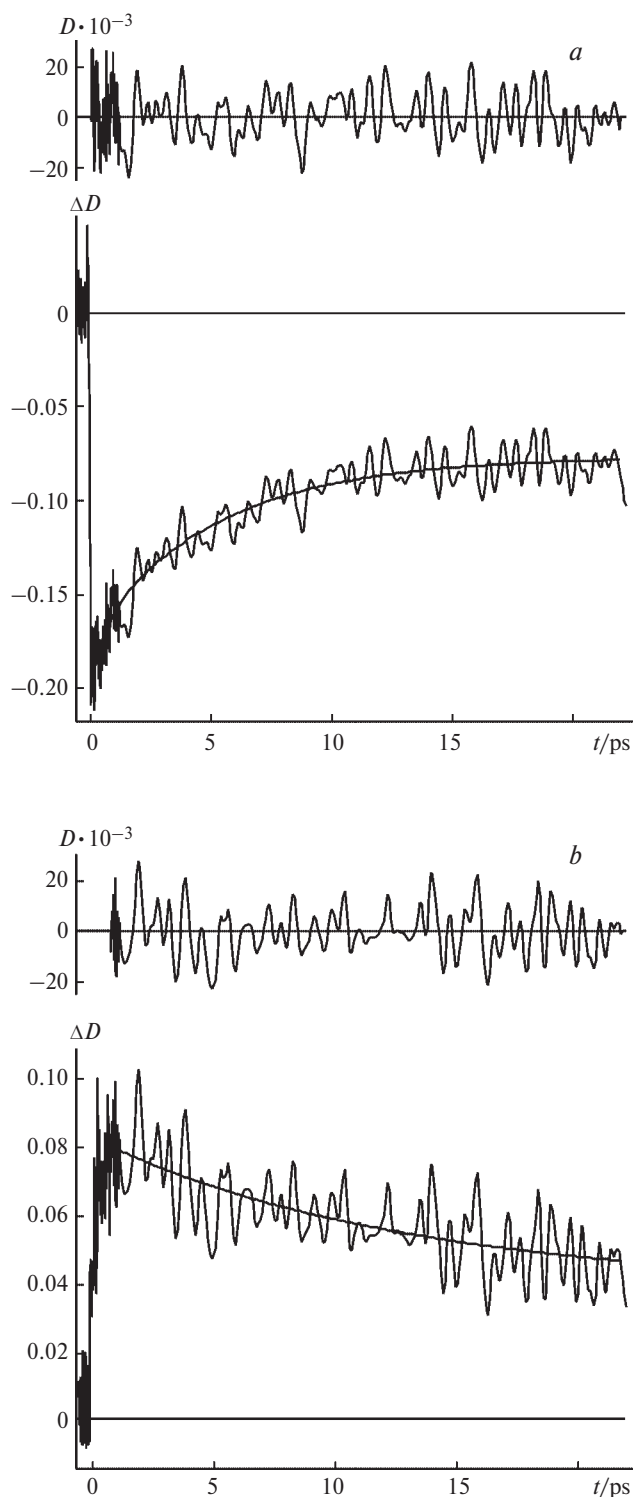


Fig. 7. Relaxation absorption curves in the picosecond time scale upon the excitation of $\text{Fc}_4\text{PH}_4^{2+}$ ($3 \cdot 10^{-5} \text{ mol L}^{-1}$) with the light pulse with $\lambda = 610 \text{ nm}$ in a $\text{CHCl}_3\text{—MeCN}$ (50 : 50, vol.%) solution at 296 K: $\lambda = 465$ (a) and 480 nm (b). The concentration of HClO_4 is $1 \cdot 10^{-3} \text{ mol L}^{-1}$. The results of approximation of the curves with the corresponding exponential functions are presented.

Table 1. Characteristic relaxation processes in the femto- and picosecond time scale for Fc_4PH_2 and $\text{Fc}_4\text{PH}_4^{2+}$

λ/nm	Type of signal ^a	Function for approximation	τ/fs
Fc_4PH_2 system			
410—425 ^b	I	$A(1 - \exp(-t/\tau))$	125 ± 30
450 ^b	II	$A(1 - \exp(-t/\tau))$	120 ± 30
410—440	I	$A + B\exp(-t/\tau)$	208 ± 10
415—435	I	$A + B\exp(-t/\tau)$	$(17 \pm 4) \cdot 10^3$
455—475	II	$A + B\exp(-t/\tau)$	$(17 \pm 3) \cdot 10^3$
$\text{Fc}_4\text{PH}_4^{2+}$ system			
485—510 ^b	I	$A(1 - \exp(-t/\tau))$	150 ± 30
435 ^b	II	$A(1 - \exp(-t/\tau))$	140 ± 40
480—550	II	$A + B\exp(-t/\tau)$	$(7.6 \pm 2.2) \cdot 10^3$
430—465	I	$A + B\exp(-t/\tau)$	$(11.4 \pm 4.4) \cdot 10^3$

^a Decay (I) or absorption (II).

^b Front edge of the signal.

ent time functions. The relaxation of Fc_4PH_2 is reflected by the biexponential function $A_1\exp(-t/\tau_1) + A_2\exp(-t/\tau_2) + B$, and that of $\text{Fc}_4\text{PH}_4^{2+}$ is described by the monoexponential function $A\exp(-t/\tau) + B$ (see Figs. 6 and 7). For Fc_4PH_2 the longer time is $\tau_2 = 17 \pm 4 \text{ ps}$ for both the decay curves with $\lambda = 415\text{—}435 \text{ nm}$ and absorption curves with $\lambda = 455\text{—}475 \text{ nm}$. The relaxation time of $\text{Fc}_4\text{PH}_4^{2+}$ for the absorption curves at 480—550 nm and decay curves with $\lambda = 430\text{—}465 \text{ nm}$ is $\tau = 9 \pm 3 \text{ ps}$ on the average (Table 1).

As indicated above, the initial excited state is $\text{Q}^1(\pi\text{—}\pi^*)$ in Fc_4PH_2 and $\text{Fc}_4\text{PH}_4^{2+}$ after light excitation with $\lambda = 610 \text{ nm}$ (16400 cm^{-1}), and its relaxation can be considered qualitatively on the basis of the relaxation processes known in the photochemistry. Let us exclude from consideration the following relaxation mechanisms.

1. The energy transfer from the $\text{Q}^1(\pi\text{—}\pi^*)$ level to the Fc levels because the energy of the lowest singlet state is $E(\text{S}_1\text{Fc}) = 18900 \text{ cm}^{-1}$ and the energy of the excited photon is 16400 cm^{-1} .

2. Heavy atom effect. In order to reveal the role of this effect, we studied the fluorescence of related *meso*-tetrametallocenylporphyrins Rc_4PH_2 and Cym_4PH_2 . These porphyrins were established to fluoresce with a much higher quantum yield than Fc_4PH_2 : $\phi_{\text{Rc}_4\text{PH}_2} = 2.8 \cdot 10^{-4} \phi_{\text{H}_2\text{TTP}}$, $\phi_{\text{Cym}_4\text{PH}_2} = 1.8 \cdot 10^{-3} \phi_{\text{H}_2\text{TTP}}$. If the quenching mechanism through a heavy atom operated, Mn in Cym_4PH_2 and Ru in Rc_4PH_2 would appear approximately the same or even higher efficiency of the $\text{Q}^1(\pi\text{—}\pi^*)$ state quenching, taking into account the higher charge of the nucleus of Ru in Rc_4PH_2 than that of Fe in Fc_4PH_2 . The quantum yield of fluorescence for Fc_4PH_2 is almost 28 times lower than that for Rc_4PH_2 . Therefore, the heavy atom effect seems an improbable mechanism for the $\text{Q}^1(\pi\text{—}\pi^*)$ state relaxation.

3. Intra- and intersystem crossing from the $Q^1(\pi-\pi^*)$ state to the ground or triplet state due to the conformational distortion of the porphyrin ring. This mechanism of acceleration of crossing transitions in porphyrins and their complexes has been considered previously.^{14,15} In our case, this mechanism is necessary to be discussed because the conformational distortions of the porphyrin ring in Fc_4PH_2 and $Fc_4PH_4^{2+}$ are indicated by several characteristic properties in the 1H NMR spectra (see Ref. 9) (chemical shift of protons of the NH group at δ 0.5, see Fig. 2, *a*) and in the absorption and fluorescence spectra^{9,10}: (a) low quantum yield of fluorescence, (b) considerable bathochromic shift of the B and Q bands of Fc_4PH_2 and $Fc_4PH_4^{2+}$ relative to the B and Q bands of the planar H_2TPP porphyrin, and (c) great Stokes shift of 1440 cm^{-1} between the absorption and fluorescence bands of $Fc_4PH_4^{2+}$ (for H_2TPP this value is equal to 142 cm^{-1}). However, the published data on porphyrins with the certainly distorted porphyrin ring show that the characteristic time of the nonradiative intersystem transition from the $Q^1(\pi-\pi^*)$ state is ≥ 300 ps.¹⁴ This time is by >1000 times longer than $\tau = 125 \pm 30$ fs and $\tau = 208 \pm 10$ fs found in this work. Therefore, it is improbable that the femtosecond relaxation processes observed are related, in our case, to intra- or intersystem crossing.

Among possible electron transitions, which could be attributed to the femtosecond relaxation of the $Q^1(\pi-\pi^*)$ state, we have the transition from the $Q^1(\pi-\pi^*)$ level to the $Fc^{\delta+}-P^{\delta-}$ charge-transfer state.¹⁰ Along with this, the relaxation processes observed can be related to the conformational and intra- and intermolecular relaxation of the vibrational energy of the $Q^1(\pi-\pi^*)$ state and/or to the intramolecular transitions between the electronic states. The vibrational relaxation of metalloporphyrins in solutions occurs in the time scale shorter than ≤ 10 ps.¹⁶⁻¹⁹ Note that the initial conditions on the vibrational energy excess for the $Q^1(\pi-\pi^*)$ state for the both Fc_4PH_2 and $Fc_4PH_4^{2+}$ porphyrins are approximately the same. As can be seen in Fig. 1, the red limit of the absorption spectra of Fc_4PH_2 and $Fc_4PH_4^{2+}$ is close to 770 and 740 nm, respectively, and the energy of the $Q^1(\pi-\pi^*)$ state is close to 13000 and 13500 cm^{-1} . The vibrational energy excess for excitation with the light with $\lambda = 610$ nm in the $Q^1(\pi-\pi^*)$ state for $Fc_4PH_4^{2+}$ is 2900 cm^{-1} , and that for Fc_4PH_2 is 3400 cm^{-1} . The process with the characteristic time $\tau = 125 \pm 30$ fs, which is observed for both systems (Fc_4PH_2 and $Fc_4PH_4^{2+}$), can be attributed to vibrational relaxation of the $Q^1(\pi-\pi^*)$ state. Taking into account the closeness of the Fc_4PH_2 and $Fc_4PH_4^{2+}$ molecular structures, not a great difference in the numbers of vibrational degrees of freedom, and the comparable energy excess, one should expect the close dynamics of vibrational relaxation. Based on these qualitative concepts, the process with $\tau = 125 \pm 30$ fs should be attributed to vibrational relaxation. As a con-

sequence of vibrational relaxation, the corresponding changes in the Franck-Condon factor should occur in the absorption cross section, which results in the transition processes observed in the differential absorption curves.

The femtosecond relaxation of Fc_4PH_2 includes the component with the characteristic time $\tau = 208 \pm 10$ fs, which is absent from $Fc_4PH_4^{2+}$ (see Figs. 4 and 5). The question arises: is this the vibrational relaxation or relaxation associated with transitions between the electronic states of Fc_4PH_2 ? The relaxation rates for Fc_4PH_2 and $Fc_4PH_4^{2+}$ can differ: (a) rates of transition from the $Q^1(\pi-\pi^*)$ state to the $Fc^{\delta+}-P^{\delta-}$ charge-transfer state substantially differ for Fc_4PH_2 and $Fc_4PH_4^{2+}$ due to the differences between the electronic structures of Fc_4PH_2 and $Fc_4PH_4^{2+}$ and (b) for the diprotonated $Fc_4PH_4^{2+}$ form the degrees of freedom of the vibrational and conformational motion of the tetrapyrrole ring are delayed due to protonation. The data presented above on the quantum yield of fluorescence for Fc_4PH_2 and $Fc_4PH_4^{2+}$ and the estimates of the rate of nonradiative transitions indicate that relaxation with $\tau = 208 \pm 10$ fs for Fc_4PH_2 is related to the transition from the $Q^1(\pi-\pi^*)$ state to the $Fc^{\delta+}-P^{\delta-}$ charge-transfer state. Relaxation with $\tau = 9 \pm 3$ ps for $Fc_4PH_4^{2+}$ is associated with the transition to the charge-transfer state for the protonated form. Vibrational relaxation itself can hardly influence so strongly on the quantum yield of fluorescence.

We studied the 1H NMR spectra to elucidate the problem about the conformational mobility of the porphyrin ring in Fc_4PH_2 and $Fc_4PH_4^{2+}$. The data obtained show that in $Fc_4PH_4^{2+}$, unlike Fc_4PH_2 , conformational motions attributed to the deformation of the porphyrin ring are frozen in the NMR time scale. In fact, as can be seen in Fig. 2, *b*, the spectrum of $Fc_4PH_4^{2+}$ at 300 K in the region of appearance of protons of the substituted Cp

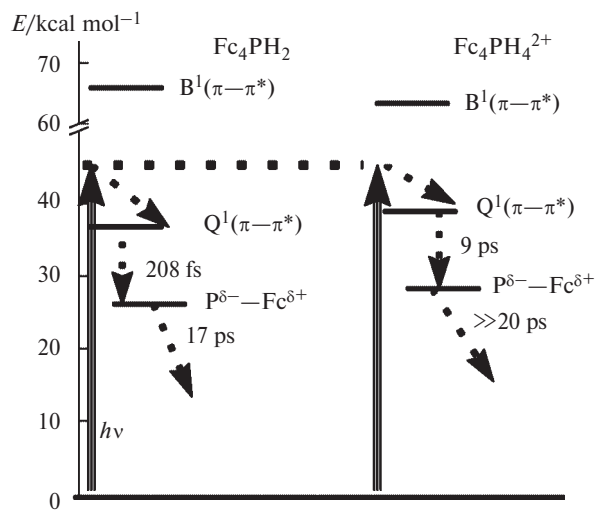


Fig. 8. Scheme of transitions for Fc_4PH_2 and $Fc_4PH_4^{2+}$.

rings (δ 4.5–6) exhibits the doubled (compared with the spectrum of Fc_4PH_2) number of signals indicating that protons in both the 2,5- and 3,4-positions of the C_5H_4 group are nonequivalent. The equal intensities of these signals and the experimental data on the spin population transfer indicate the existence of a degenerate equilibrium between protons in positions 2 and 5 and also 3 and 4. On the contrary, in the case of nonprotonated porphyrin, the spectral pattern does not substantially change in the 350–220 K temperature interval. We cannot exclude that the mobility of the porphyrin ring in Fc_4PH_2 promotes the very fast (208 ± 10 fs) transition from the $\text{Q}^1(\pi-\pi^*)$ state to the $\text{Fc}^{\delta+}-\text{P}^{\delta-}$ charge-transfer state. It has previously¹⁹ been shown that the mobility of the ring can accelerate transitions between electronic states in porphyrins. Regarding Fc_4PH_2 , this problem needs additional studies.

The transitions occurring upon the photoexcitation of Fc_4PH_2 and $\text{Fc}_4\text{PH}_4^{2+}$ are presented in Fig. 8.

This work was financially supported by the Russian Foundation for Basic Research (Project Nos. 98-03-33187 and 00-03-40118).

References

1. K. I. Zamaraev and R. F. Khairutdinov, *Top. Curr. Chem.*, 1992, **163**, 1.
2. M. N. Paddon-Row, *Acc. Chem. Res.*, 1994, **27**, 18.
3. S. Priyadarshy, M. J. Therien, and D. N. Beratan, *J. Am. Chem. Soc.*, 1996, **118**, 1504.
4. M. P. O'Neil, M. P. Niemczyk, W. A. Svec, D. Cosztola, G. L. Gaines, III, and M. R. Wasielewski, *Science*, 1992, **257**, 63.
5. L. Karki, F. W. Vance, J. T. Hupp, S. M. LeCours, and M. J. Therien, *J. Am. Chem. Soc.*, 1998, **120**, 2606.
6. *Photodynamic Therapy of Neoplastic Diseases*, Ed. D. Kessel, CRC Press, Boca Raton, FL, 1990, **I, II**.
7. K. Uosaki, T. Kondo, Xue-Qun Zhang, and M. Yanagida, *J. Am. Chem. Soc.*, 1997, **119**, 8367.
8. N. M. Loim, N. A. Abramova, and V. I. Sokolov, *Mendeleev Commun.*, 1996, 46.
9. N. M. Loim, N. V. Abramova, R. Z. Khaliulin, Yu. S. Lukashov, E. V. Vorontsov, and V. I. Sokolov, *Izv. Akad. Nauk, Ser. Khim.*, 1998, 1045 [*Russ. Chem. Bull.*, 1998, **47**, 1016 (Engl. Transl.)].
10. V. A. Nadochenko, N. N. Denisov, V. Yu. Gak, N. V. Abramova, and N. M. Loim, *Izv. Akad. Nauk, Ser. Khim.*, 1999, 1924 [*Russ. Chem. Bull.*, 1999, **48**, 1900 (Engl. Transl.)].
11. J. Rodriguez, C. Kirmier, and D. Holten, *J. Am. Chem. Soc.*, 1989, **111**, 6500.
12. F. E. Gostev, A. A. Kachanov, and S. A. Kovalenko, *Instrum. Experim. Techn.*, 1996, **39**, 567.
13. R. D. Rihter, M. D. Bohorquez, M. A. J. Rodgers, and M. E. Kenney, *J. Chem. Soc., Faraday Trans. 2*, 1994, **90**, 1073.
14. S. Gentemann, J. Medforth, T. Forsyth, D. J. Nurco, K. M. Smith, K. Fajer, and D. Holten, *J. Am. Chem. Soc.*, 1994, **116**, 7363.
15. C. M. Drain, C. Kimaier, C. J. Mesdforth, D. J. Nurco, K. M. Smith, and D. Holten, *J. Phys. Chem.*, 1996, **100**, 11984.
16. T. Kobayashi, K. D. Straub, and P. M. Rentzepis, *Photochem. Photobiol.*, 1979, **29**, 925.
17. V. S. Chirvonyi, B. M. Dzhagarov, Y. V. Timinskii, and G. P. Gurinovich, *Chem. Phys. Lett.*, 1980, **70**, 79.
18. D. Kim, C. Kirmaier, and D. Holten, *Chem. Phys.*, 1983, **91**, 3225.
19. C. M. Drain, S. Gentemann, J. A. Roberts, N. Y. Nelson, C. J. Medforth, S. Jia, M. C. Simpson, K. M. Smith, J. Fajer, J. A. Shelnutt, and D. Holten, *J. Am. Chem. Soc.*, 1998, **120**, 3781.

Received July 18, 2001;
in revised form January 25, 2002